Fractal Particle Trajectories in Capillary Waves: Imprint of Wavelength

Adam E. Hansen, Elsebeth Schröder, Preben Alstrøm, Jacob Sparre Andersen, and Mogens T. Levinsen
Center for Chaos and Turbulence Studies, The Niels Bohr Institute, Blegdamsvej 17, DK-2100 Copenhagen Ø, Denmark
(Received 2 December 1996; revised manuscript received 26 June 1997)

We examine particle trajectories in capillary waves formed on a water surface subject to vertical vibrations. We focus on the role of a distinct length scale present in our experiment, namely, the wavelength λ of the surface waves. We observe non-Brownian particle trajectories with a fractal dimension D different from the random walk value $D = 2$. A crossover is observed from one anomalous behavior at length scales below λ, to another at larger length scales. Data collapse is shown to be feasible, and scaling functions characterizing the crossover are identified. Our results are compared to those obtained from observations of drifters in the upper ocean. The distinct length scale λ allows us to divide the particle trajectories into flights and traps. The distribution of flight times shows a power-law behavior with an exponent between 2.3 and 3. [S0031-9007(97)04033-7]

PACS numbers: 47.20.Dr, 05.40.+j, 47.27.Qb, 47.52.+j

Studies of the turbulent motion of drifters in the upper ocean [1–3] have shown that the drifter motion possesses a significant persistence, which is not present in ordinary Brownian motion. Rather, the motion seems to be better described as a fractional Brownian motion with anomalous dispersion properties. For example, for $x(t)$ being one component of the horizontally projected drifter trajectory $\mathbf{r}(t) = [x(t), y(t)]$, the single particle dispersion $V(\tau) = \langle [x(t + \tau) - x(t)]^2 \rangle$ increases as a power law in time τ, $V(\tau) \sim \tau^{2H}$, where the "fractional Brownian motion" exponent $2H$ is larger than the unit value found for ordinary Brownian motion. Also, the fractal dimension D for the drifter trajectories has been determined based on the "yardstick method" [4], and the value obtained for D is significantly smaller than the Brownian motion result $D = 2$, and in good agreement with the value $D = 1/H$ derived for a fractional Brownian motion [4]. Moreover, the values of H and D reported for different geographic locations are found to have surprisingly little variation.

In the experiment reported here the motion of particles on surface waves is studied on much smaller time and length scales than those considered in the upper-ocean studies. The surface waves are formed in a cylindrical container (interior diameter = 8.4 cm and height = 2 cm) filled with water to a height of approximately 1 cm, and vertically vibrated at a frequency of 260 Hz. At vibration amplitudes A above a critical amplitude A_c, capillary surface waves are formed with a wavelength λ of approximately 2.6 mm. The particles used were mushroom spores of size $\sim$50 μm. The motion of the particles was recorded by a charge-coupled device (CCD) camera to a VCR sampling at 50 Hz, thus storing the horizontal position of the particles at 20 ms intervals [5]. Thousands of particle trajectories were in this way collected and analyzed for seven different values of the reduced control parameter $\epsilon = (A - A_c)/A_c$, ranging from $\epsilon = 0.05$ to $\epsilon = 1.06$. The trajectories were obtained on a time scale from 20 ms to 30 s and a length scale from 0.1 to 50 mm. Two examples of trajectories are shown in Fig. 1.

Measurements on single particle dispersion in capillary surface waves have previously been analyzed on a time scale above 1 s by Ramshankar, Berlin, and Gollub (RBG) [6]. On a time scale of approximately 1 s the particle is found to move a wavelength or so, the distance increasing with the value of ϵ. In the regime above this time and length scale, the single particle dispersion exponent $2H$ is found to vary from $2H \sim 1.3$ at small values of ϵ to the Brownian value $2H = 1$ at larger values of ϵ.

In the present experiment both the particle dispersion exponent $2H$ and the fractal dimension D of our particle trajectories are determined. Moreover, we take the analysis to smaller time and length scales. Although the turbulent flow may show an almost Brownian particle dispersion at large length scales, there is still a distinct length scale in the fluid system, namely, the wavelength λ. It is insufficient to describe the particle motion in terms of a single fractional Brownian motion characterized only by the exponent $2H \sim 1.0$–1.3 when length scales both smaller and

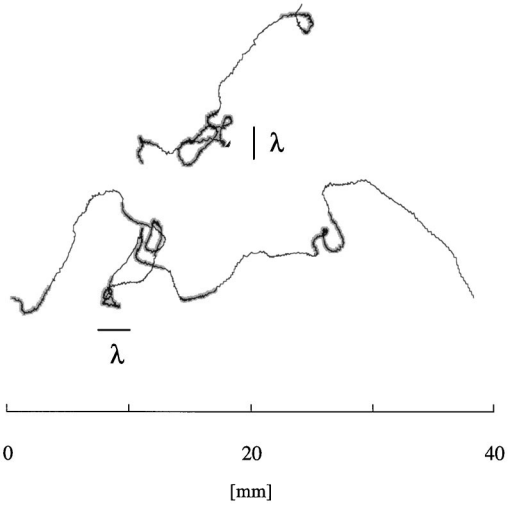

FIG. 1. Two particle trajectories for $\epsilon = 0.05$ divided into flights (thin lines) and traps (thick lines).

larger than the wavelength λ are taken into account. Our experiment addresses this point. How does the flow on large length scales relate to the flow on small length scales? Our results show that the description of the particle motion as a fractional Brownian motion at length scales above the wavelength can be extended to all length scales by convoluting the motion with another fractional Brownian motion that has a persistence length limited to the wavelength. We find the latter motion to be characterized by a universal exponent $2H_\lambda \simeq 1.55$ and a fractal dimension $D_\lambda \simeq 1.3$, surprisingly independent of the vibration amplitude. A scaling function is identified, which significantly extends the scaling range over which the exponent $2H$ is determined.

Figure 2(a) shows the variance $V(\tau)$ obtained for seven values of ϵ, $0.05 \leq \epsilon \leq 1.06$. There was no preference for any spatial direction in the horizontal plane. The variance obtained by projecting the horizontal motion $\mathbf{r}(t)$ onto two perpendicular directions $x(t)$, $y(t)$ we found (as RBG) to be the same. The dotted horizontal line in Fig. 2(a) is where $V(\tau) = \lambda^2/2$, and the times $\tau_c(\epsilon)$ at which the curves cross this line are the characteristic times associated with the distinct length scale λ. All curves show a crossover at this length scale from one behavior above λ, where the particle motion at large ϵ becomes Brownian, to a steeper power-law behavior at length scales smaller than λ. The crossover time τ_c decreases with growing vibration amplitude; the particles simply move faster for higher amplitudes. The decay of τ_c is approximately exponential in ϵ, $\tau_c(\epsilon) \simeq \tau_c(0)\exp(-1.8\epsilon)$, where $\tau_c(0) \simeq 600$ ms [inset of Fig. 2(a)]. We notice that $\tau_c(0)$ is more than 2 orders of magnitude smaller than the molecular diffusion time associated with λ.

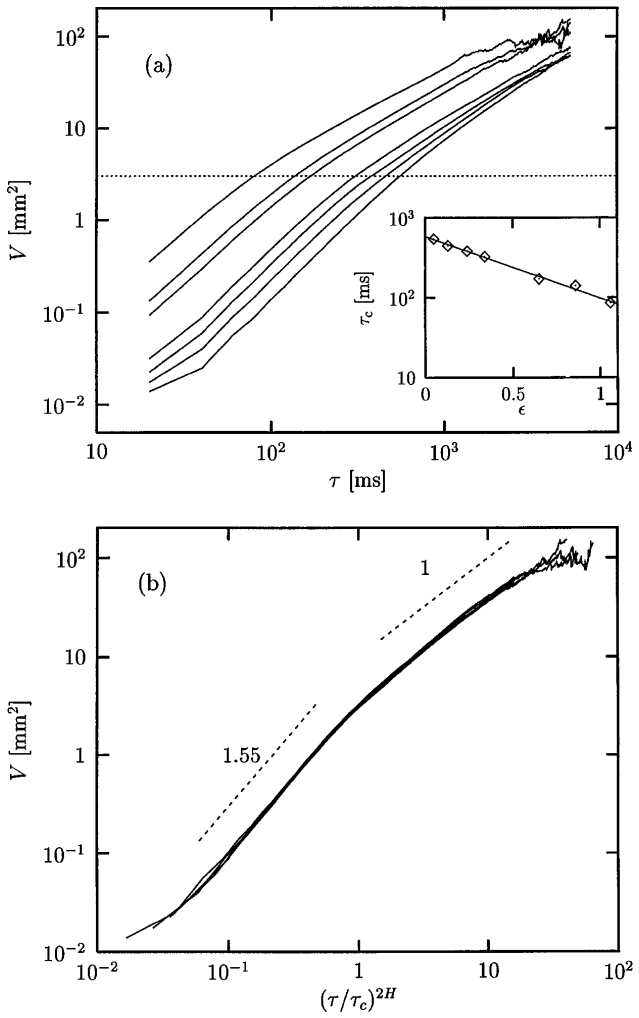

FIG. 2. (a) Variance $V(\tau)$ obtained for $\epsilon = 0.05$, 0.13, 0.24, 0.34, 0.65, 0.86, and 1.06 (top curve). The dotted horizontal line is where $V(\tau) = \lambda^2/2$. The times at which the curves cross this line are denoted $\tau_c(\epsilon)$. Inset: The decay of $\tau_c(\epsilon)$ is approximately exponential, $\tau_c(\epsilon) \simeq \tau_c(0)\exp(-1.8\epsilon)$. (b) The dispersion curves shown in (a) are collapsed into a scaling function by rescaling the curves according to an ϵ-dependent exponent $2H$, where H is given in Table I.

In order to determine the "large-scale" exponent $2H$ for the variance (scales larger than λ), we first normalized the time by the characteristic time $\tau_c(\epsilon)$. Second, we rescaled this dimensionless time by an exponent $2H(\epsilon)$. For $\epsilon = 1.06$ the exponent was identified to have the Brownian motion value 1. Assuming that the variance scales as $V(\tau) \sim \tau^{2H}$, we expect the data to collapse at length scales above λ if the values of $2H$ are correctly chosen (Table I). Indeed, the data collapse is very good [Fig. 2(b)]. However, we not only find data collapse above λ. The data collapse extends over the entire scaling regime. The scaling function obtained shows a crossover from one power-law behavior characterized by the exponent $2H_\lambda = 1.55 \pm 0.05$ to the behavior of an ordinary Brownian motion ($2H = 1$). Such a behavior can be modeled by a fractional Brownian motion with a limited persistence imposed. The existence of a scaling function across the entire time regime studied provides a more accurate estimate of the exponent $2H(\epsilon)$, compared to estimating a large-scale exponent directly from Fig. 2(a) (or from the corresponding curves in RBG).

The higher moments $\langle[x(t+\tau) - x(t)]^n\rangle$ for the particle dispersion were also considered. An analysis similar to the above shows that the nth absolute moment scales as $V(\tau)^{\zeta_n}$, where ζ_n is found to be very close to $n/2$. However, a more detailed analysis of deviations from a Gaussian behavior gave some further insight. In particular, we find generally that the skewness (derived from the third moment) changes sign, from being positive at time

TABLE I. The values of $H(\epsilon)$, $1/H(\epsilon)$, and $D(\epsilon)$ obtained by rescaling.

ϵ	$H(\epsilon)$	$1/H(\epsilon)$	$D(\epsilon)$
0.05	0.63	1.59	1.65
0.13	0.59	1.69	1.72
0.24	0.57	1.77	1.76
0.34	0.55	1.82	1.81
0.65	0.54	1.87	1.89
0.86	0.53	1.87	1.95
1.06	0.50	2.00	2.00

scales below τ_c to being negative at time scales above τ_c. This emphasizes the presence of two dynamically distinct diffusion processes, one of them having the persistence length λ. In addition, the kurtosis (derived from the fourth moment) is found always to be positive on all scales, however, decreasing with increasing τ. Thus the underlying distribution becomes flatter at larger scales, as is usually the case for turbulent motion. The deviation from a Gaussian distribution is more pronounced at larger forcings (larger ϵ).

Next, we determine the fractal dimension of our trajectories. The trajectories are defined by linear interpolation between successive data points. We apply the standard "yardstick" method [4], where the length of the trajectory is measured on various scales η. The fractal dimension D of the trajectory is defined from the number $N(\eta)$ of yardsticks used, $N(\eta) \sim \eta^{-D}$. For ordinary Brownian motion $D = 2$, while $D = 1/H < 2$ for persistent fractional Brownian motion. Figure 3 shows our results for $N(\eta)$. In the plot the scale η is measured in units of the wavelength λ, and the number N of yardsticks is normalized to the number obtained at $\eta = \lambda$. To find $N(\eta)$, we constructed one long "trajectory" by translating the trajectories so that the end point of one trajectory was identified with the starting point of another. Naturally, the scale η must be chosen smaller than the typical size of a single track. The maximal value of scale in Fig. 3 is set to $\eta_{\max} = 10$ mm. At $\eta_{\max}$, 90% of the trajectories have a size larger than this scale. The lower scale limit $\eta_{\min}$ (the smallest yardstick used) is set by the typical distance between two successive data points, i.e., the typical distance a particle moves in 20 ms. More precisely, $\eta_{\min}$ is defined as the scale where 90% of the distances between successive data points are less than $\eta_{\min}$. Since particles move faster at larger values of ϵ, $\eta_{\min}$ increases with ϵ.

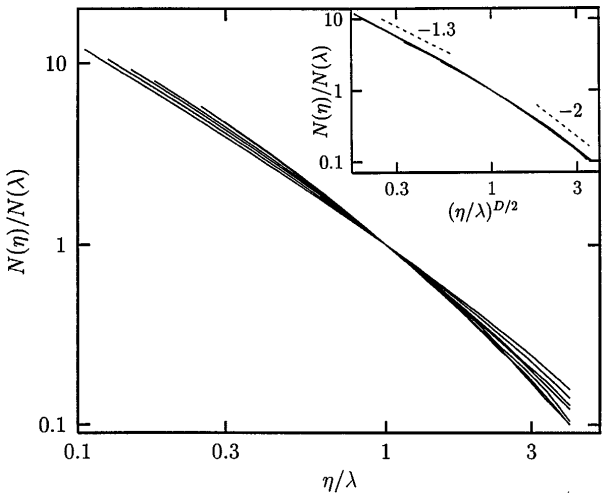

FIG. 3. Number $N(\eta)$ of yardsticks used to follow the particle trajectories on scale η, normalized to the number used at $\eta = \lambda$ (log-log plot). The curves show $N(\eta)$ for $\epsilon = 0.05$, 0.13, 0.24, 0.34, 0.65, 0.86, and 1.06 (steepest curve). The scale η is measured in units of the wavelength λ. Inset: The $N(\eta)$ curves are collapsed into a scaling function by rescaling the curves according to an ϵ-dependent exponent $D/2$, where D is given in Table I.

The curves in Fig. 3 can be collapsed into one by rescaling the scale η by an ϵ-dependent exponent $D(\epsilon)/2$, where $D = 2$ for the largest value of ϵ (inset of Fig. 3). We find that the obtained value of $D(\epsilon)$ is in good agreement with the estimate $1/H(\epsilon)$ of the fractal dimension obtained from the single particle dispersion (Table I). Again the data collapse extends across the wavelength scale. The scaling function obtained shows a crossover from a power-law behavior characterized by the exponent $D_\lambda = 1.30 \pm 0.05$ to the behavior of an ordinary Brownian motion ($D = 2$). We note that $D_\lambda = 1/H_\lambda$.

In upper-ocean studies of the motion of drifters [1–3], the time scales and length scales considered are of order 1–10 days and 10–100 km, respectively. Both the dispersion exponent H and the fractal dimension D have been determined. The values of H and D reported from different geographic locations are found to have surprisingly little variation. The values $2H \sim 1.5$–1.6 and $D \sim 1.3$ are found in the northeast Atlantic Ocean (Rockall Trough) [1], in the northwest Atlantic Ocean (Conception Bay, Newfoundland) [2], and in the Pacific Ocean near Japan (Kuroshio extension) [3]. Moreover, the relation $D = 1/H$ seems to hold quite well. It is intriguing that (but unclear why) the observed upper-ocean values of H and D are the same as the small length-scale results H_λ and D_λ that we obtain for large vibration amplitudes [see the scaling functions in Fig. 2(b) and the inset of Fig. 3]. In the present experiment the crossover to ordinary Brownian motion is observed at the wavelength scale. In upper-ocean studies the corresponding crossover scale is more than 100 km, at which the dynamics is governed by Rossby waves and zonal flows (the largest eddies) [3].

The exponent $2H \sim 1.5$–1.6 obtained from ocean studies has also been associated with numerical results obtained for vortex trajectories in two-dimensional turbulence [7,8]. In this connection, the exponent ξ characterizing the decay of the vortex density ρ in freely evolving two-dimensional turbulence, $\rho \sim t^{-\xi}$, seems to be important. The value of ξ is found to be $\xi \simeq 0.75$ [9], and quite universal [10]. He [8] has suggested the relation $2H = 2 - \frac{1}{2}\xi$. Using $\xi = 0.75$, the value $2H = 1.63$ is obtained. Whether the above relations apply for our forced system or for the barotropic turbulent flow studied by Elhmaïdi *et al.* [7] needs a more analytical consideration.

The distinct length scale λ and corresponding time scale $\tau_c(\epsilon)$ allow us to consider the particle motion as a chaotic advection process with traps and flights. For this purpose, we associate with each data point $\mathbf{r}(t)$ along a particle track, a "velocity" $v[\mathbf{r}(t)] = |\mathbf{r}[t + (\tau_c/2)] - \mathbf{r}[t - (\tau_c/2)]|/\tau_c$. The particle tracks are now divided into flights and traps according to the following procedure: (i) Data points with $v(\mathbf{r}) > \lambda/\tau_c$ are denoted "flight points"; those with $v(\mathbf{r}) \leq \lambda/\tau_c$ are denoted

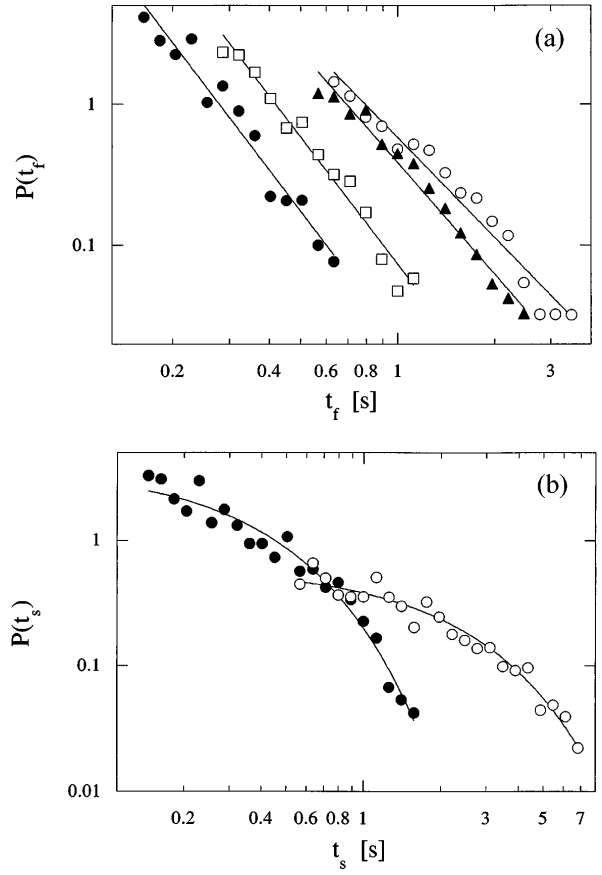

FIG. 4. (a) Double-logarithmic plot of the distribution of flight times, $P(t_f)$, for $\epsilon = 0.05$ (∘), $\epsilon = 0.24$ (triangles), $\epsilon = 0.65$ (squares), and $\epsilon = 1.06$ (•). The straight lines have absolute slope $\mu = 2.3$, $\mu = 2.6$, $\mu = 3.0$, and $\mu = 3.0$. (b) Corresponding plot of the distribution of sticking times, $P(t_s)$, obtained for $\epsilon = 0.05$ (∘), and $\epsilon = 1.06$ (•).

"sticking points." (ii) If a sequence of sticking points between two flight points corresponds to a time span less than τ_c, the sticking points are changed into flight points. Thus, a particle is only considered trapped if sticking is observed for a period longer than τ_c. (iii) If a sequence of flight points between two sticking points is so short that the particle has moved a distance less than λ, the flight points are changed into sticking points. Thus, to escape a trap, a particle must "fly" farther than a wavelength. (iv) Consecutive sticking points are now called a trap, and consecutive flight points are called a flight. Traps and flights at the ends of a trajectory are discarded [11]. By definition, traps last longer than τ_c, and flights are over distances larger than λ. The division of trajectories into flights and traps are illustrated in Fig. 1, showing that the trapped motion is nontrivial and possibly very influenced by the weakly turbulent motion of the underlying pattern.

We have determined the flight time and sticking time distributions (normalized), $P(t_f)$ and $P(t_s)$; see Figs. 4(a) and 4(b). The distributions are cut off at $P(t) = 0.005$. Beyond this point, the distributions are heavily influenced by the finite duration of the measured trajectories [11]. If a power-law behavior is assumed for the flight times [Fig. 4(a)], $P(t_f) \sim t_f^{-\mu}$ [12], we find μ to increase from $\mu = 2.3$ to $\mu = 3$ for increasing values of ϵ. In comparison, the proposed relation $\mu = 4 - 2H$ [12] between the advection exponent μ and the diffusion exponent $2H$ yields a μ value changing from $\mu = 2.7$ to $\mu = 3$ for increasing values of ϵ. The distribution of sticking times, $P(t_s)$, seems to be exponentially decaying rather than to follow a power law [Fig. 4(b)]. This suggests that the anomalous diffusion is dominated by the flight time statistics.

In conclusion, we have shown that data obtained for single particle dispersion in capillary waves for different values of the vibration amplitude can be collapsed over a wide scaling regime that includes the wavelength scale. The fractal particle motion previously reported at length scales above the wavelength [6] can be extended to all length scales by convoluting the motion with another fractional Brownian motion with a persistence length equal to the wavelength. This latter motion is characterized by the universal exponents $2H_\lambda \simeq 1.55$ and $D_\lambda \simeq 1.3$. These values are surprisingly the same as those generally found for fractal drifter trajectories in the upper ocean. Finally, we have analyzed the fractal particle trajectories in terms of flights and traps, revealing a power-law distribution of flight times, and a highly nontrivial trapped motion.

We are indebted to Walter Goldburg for his experimental help. The research was supported by the Novo-Nordisk Foundation and by the Danish Natural Science Research Council.

[1] B. G. Sanderson and D. Booth, Tellus **43A**, 334 (1991).
[2] B. de Young and B. Sanderson, Atmos. Ocean **33**, 135 (1995).
[3] A. R. Osborne, A. D. Kirwan, Jr., A. Provenzale, and L. Bergamasco, Tellus **41A**, 416 (1989).
[4] See, e.g., B. B. Mandelbrot, *The Fractal Geometry of Nature* (Freeman, San Francisco, 1982).
[5] A more detailed description of the general experimental setup and the tracking program can be found in P. Alstrøm, J. S. Andersen, W. I. Goldburg, and M. T. Levinsen, Chaos Solitons Fractals **5**, 1455 (1995).
[6] R. Ramshankar, D. Berlin, and J. P. Gollub, Phys. Fluids A **2**, 1955 (1990).
[7] D. Elhmaïdi, A. Provenzale, and A. Babiano, J. Fluid Mech. **257**, 533 (1993).
[8] X. He, Physica (Amsterdam) **95D**, 163 (1996).
[9] G. F. Carnevale, J. C. McWilliams, Y. Pomeau, J. B. Weiss, and W. R. Young, Phys. Rev. Lett. **66**, 2735 (1991).
[10] G. Huber and P. Alstrøm, Physica (Amsterdam) **195A**, 448 (1993).
[11] T. H. Solomon, E. R. Weeks, and H. L. Swinney, Physica (Amsterdam) **76D**, 70 (1994).
[12] See, e.g., J. Klafter, A. Blumen, and M. F. Shlesinger, Phys. Rev. A **35**, 3081 (1987).